

# Characteristics of strong motions and damage implications of $M_S6.5$ Ludian earthquake on August 3, 2014

Peibin Xu · Ruizhi Wen · Hongwei Wang ·  
Kun Ji · Yefei Ren

Received: 24 September 2014 / Accepted: 5 December 2014 / Published online: 3 February 2015  
© The Author(s) 2015. This article is published with open access at Springerlink.com

**Abstract** The Ludian County of Yunnan Province in southwestern China was struck by an  $M_S6.5$  earthquake on August 3, 2014, which was another destructive event following the  $M_S8.0$  Wenchuan earthquake in 2008,  $M_S7.1$  Yushu earthquake in 2010, and  $M_S7.0$  Lushan earthquake in 2013. National Strong-Motion Observation Network System of China collected 74 strong motion recordings, which the maximum peak ground acceleration recorded by the 053LLT station in Longtoushan Town was  $949 \text{ cm/s}^2$  in E–W component. The observed PGAs and spectral ordinates were compared with ground-motion prediction equation in China and the NGA-West2 developed by Pacific Earthquake Engineering Researcher Center. This earthquake is considered as the first case for testing applicability of NGA-West2 in China. Results indicate that the observed PGAs and the 5 % damped pseudo-response spectral accelerations are significantly lower than the predicted ones. The field survey around some typical strong motion stations verified that the earthquake damage was consistent with the official isoseismal by China Earthquake Administration.

**Keywords** Ludian earthquake · Strong motion recording · GMPE · Seismic intensity · Field survey

## 1 Introduction

An earthquake occurred on August 3, 2014, at 16:30, in Ludian County of Yunnan Province and the magnitude was

$M_S6.5$  by the China Earthquake Networks Center and the hypocenter depth was 12 km. The earthquake was destructive with seismic intensity up to IX and caused 615 dead, 114 missing, and 3,143 injured (at the end of August 7, 2014). It was another shallow earthquake following the  $M_S8.0$  Wenchuan earthquake in 2008,  $M_S7.1$  Yushu earthquake in 2010, and  $M_S7.0$  Lushan earthquake in 2013 (Wen et al. 2013). This event caused exceptionally severe damages at the epicenter near Longtoushan Town in Ludian County. Destruction at this level has not been seen in the area over a decade though the similar size earthquake occurred once before.

In this earthquake, a total of 74 strong motion stations were triggered from National Strong-Motion Observation Network System (NSMONS) of China. A rare opportunity was provided to interpret the great casualty and loss for such a moderate earthquake in terms of strong-motion observation. In this paper, the maximum peak ground accelerations (PGAs) and spectral ordinates were compared with the predicted values given by the Huo89 ground-motion prediction equations (GMPEs). The Next Generation Attenuation (NGA-West2) models were released by Pacific Earthquake Engineering Researcher Center (PEER) in early 2014, and this earthquake could be considered as a case for testing applicability of NGA-West2 in China. We also investigated the earthquake damage on buildings around six typical strong motion stations in the post-earthquake field survey and managed to find the correlation between the strong motions and building damages.

## 2 Ludian earthquake sequences and strong motions

The magnitude of  $M_S6.5$  for the mainshock was measured by the China Earthquake Networks Center, and the

P. Xu · R. Wen (✉) · H. Wang · K. Ji · Y. Ren  
Institute of Engineering Mechanics, China Earthquake  
Administration, Harbin 150080, China  
e-mail: ruizhi@iem.ac.cn

magnitude of  $M_W 6.1$  was estimated by the U.S. Geological Survey. The rupture process was inverted by Hao et al. (2014) using the regional broadband waveforms and showed the strike, dip, and slip angles were  $162^\circ$ ,  $86^\circ$ , and  $6^\circ$ , respectively. The seismogenic fault was a slip–strike one, Baogunao–Xiaohe fault. The similar results given by Zhang et al. (2014) also showed that it was a slip–strike event with magnitude of  $M_W 6.3$ , the strike, dip, and slip angles were  $165^\circ$ ,  $87^\circ$ , and  $6^\circ$ , respectively. After the mainshock, total 1,335 aftershocks occurred by the end of August 11, 2014 and there were none of magnitude 5.0–5.9 event, 4 events of magnitude 4.0–4.9, 8 events of magnitude 3.0–3.9. Most of aftershocks occurred in a wide area of the surface projection of the fault plane in Fig. 1a given by Zhang et al. (2014).

We selected 68 free-field strong-motion recordings from NSMONS during the mainshock within a rupture distance ( $R_{rup}$ ) of 300 km, which  $R_{rup}$  is the distance between the site and the closest point on the rupture surface. The other recordings are too far from the fault plane, not interesting in the engineering field. Figure 1b shows the geographical locations of these stations. We processed the strong-motion recordings using the same methodology that was applied for the Wenchuan earthquake (Boore 2001; Ren et al. 2011). The baseline correction was made for some near-field recordings, and then a Butterworth filter with a 0.1–30 Hz bandwidth was applied. As a result, the processed ground motion can be considered to provide reliable estimates of PGA and the spectral ordinates. There are seven strong-motion stations within the rupture distance of 50 km, 15 stations are within the range of 50–100 km. The largest PGA was observed at the 053LLT station in

Longtoushan Town, which recorded PGAs in the east–west (E–W), north–south (N–S), and up–down (U–D) components of 949, 706, and 504  $\text{cm/s}^2$ , respectively, close to the maximum PGAs recorded at the 051WCW station in Wenchuan earthquake (957.7, 652.9, and 941.8  $\text{cm/s}^2$  in the E–W, N–S, and U–D directions, respectively).

### 3 Comparison with Chinese GMPE and NGA-West2 models

Comparison between the observed ground motions of an earthquake and the predicted values using GMPEs is of particular interest to validate regional design ground-motion levels. The observed horizontal PGAs and the 5 % damped pseudo-spectral accelerations (PSAs) at periods  $T = 0.2, 0.5, \text{ and } 1.0$  s were compared with Huo89 GMPE for southwest China as shown in Fig. 2 (Huo 1989). The rock and soil site condition defined are included in Huo89. Huo89 was developed using a transform method proposed for regions with no ground-motion data (Hu and Zhang 1983). The results show that the observed PGAs have a good consistency with the predicted values with  $R_{rup} < 100$  km, while the predicted data by Huo89 are slightly lower than the observed data when  $R_{rup}$  is greater than 100 km in terms of rock. The observed horizontal PSAs with 5 % damping ratio are also compared with the predicted values from Huo89 in terms of rock and soil for periods  $T = 0.2, 0.5, \text{ and } 1.0$  s. Considering the fact that portion of observed values are obtained from rock sites and others are obtained from soil sites, both rock and soil site conditions are chosen for calculating the predicted values.

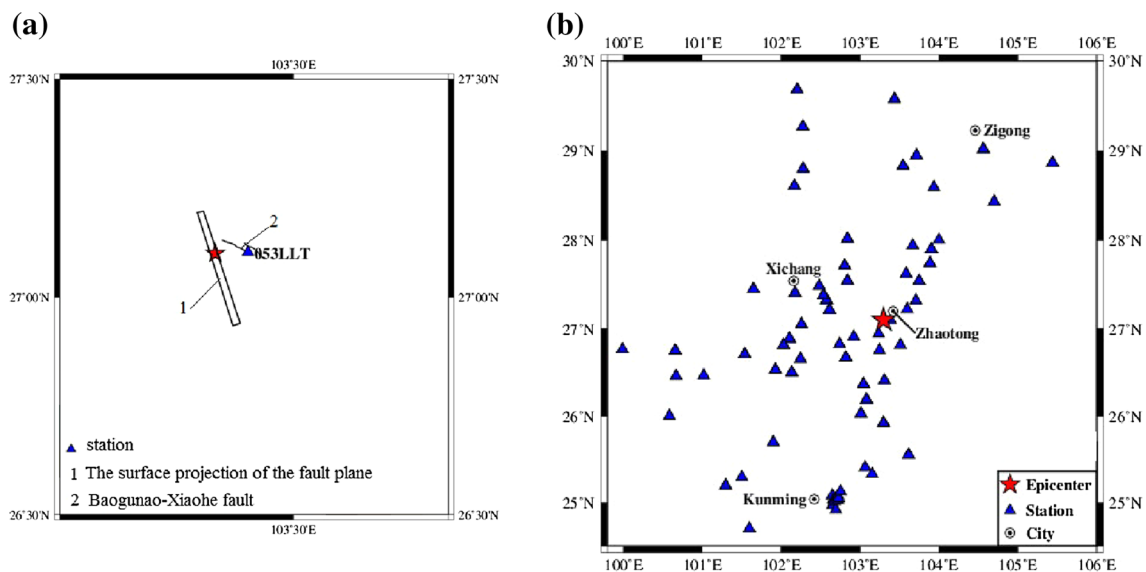


**Fig. 1** **a** Projection of the rupture plane on the surface given by Zhang et al. (2014) and the Baogunao–Xiaohe fault. **b** Locations of the free-field strong-motion stations ( $R_{rup} < 300$  km) during the Ludian earthquake

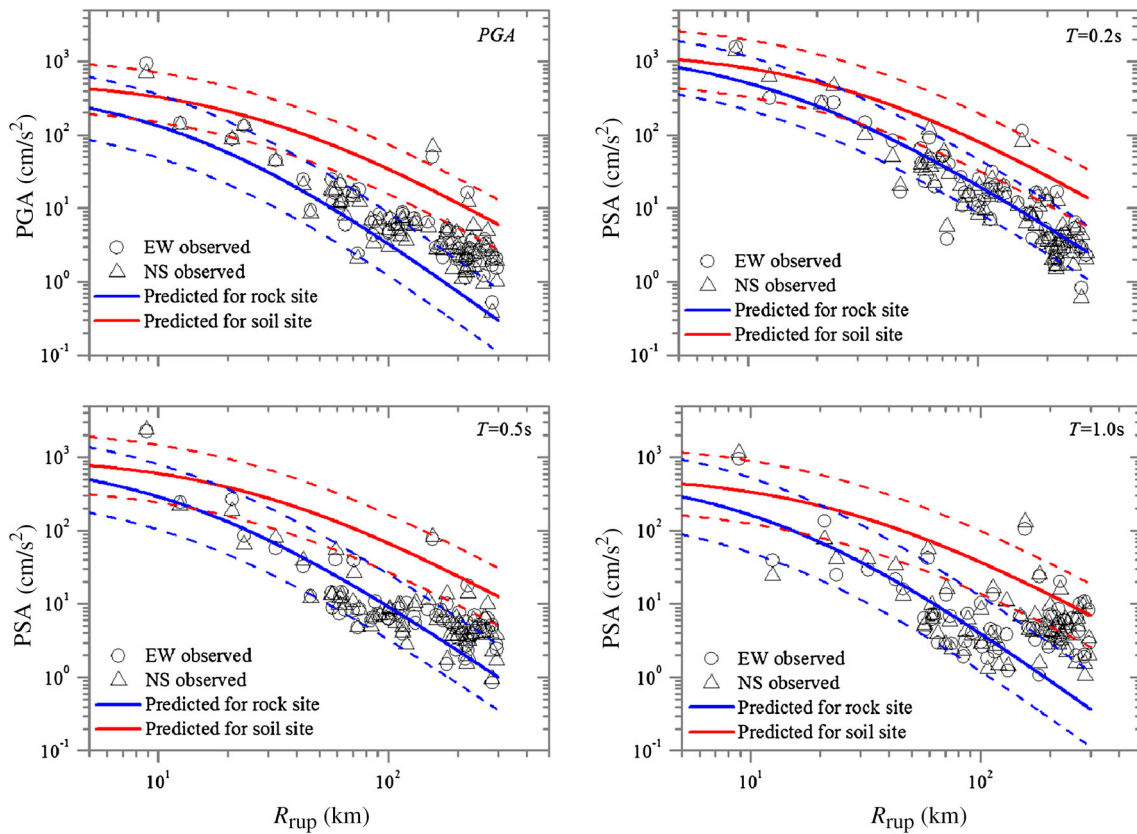


**Fig. 2** Comparison between the observed and predicted horizontal PGAs and 5 % damped pseudo-response spectral accelerations (PSAs) at periods  $T = 0.2, 0.5,$  and  $1.0$  s calculated using the Huo89 GMPE for the rock and soil site, respectively. The *dashed line* denotes the one standard deviation range

Most of the observed PSAs at short and medium periods of 0.2 and 0.5 s are within one standard deviation from the predicted values in terms of the rock site. However, for longer period of 1.0 s, the GMPE matches the observed values well with  $R_{rup} < 100$  km but underestimates the data with  $R_{rup} > 100$  km in terms of the rock site. The observed PGAs and PSAs ( $T = 0.2, 0.5,$  and  $1.0$  s) are lower than the predicted values in terms of the soil site.

The NGA-West2 project is a large multidisciplinary, multi-year research program on the next generation attenuation models for shallow crustal earthquakes in active tectonic regions. Five GMPEs for the horizontal component of ground motion have been developed in this project which supersede the NGA-West1 2008 version and released the latest one (NGA-West2) (Gregor, et al. 2014). The five GMPEs are ASK14 (Abrahamson et al. 2014), BSSA14 (Boore et al. 2014), CB14 (Campbell and Bozorgnia 2014), CY14 (Chiou and Youngs 2014), and I14 (Idriss 2014). The Ludian earthquake provided a good opportunity to examine applicability of NGA-West2 models in southwestern China. Figure 3 presents comparisons between the observed PGAs and PSAs at periods

$T = 0.2, 0.5,$  and  $1.0$  s and the five GMPEs in NGA-West2. Appropriate distance and site condition represented with average uppermost 30 m shear-wave velocity ( $V_{S30}$ ) are taken into the five GMPEs. The  $V_{S30}$  values of some stations are determined by the borehole data, and the others are derived from the recommended values in NGA-West2 database. Joyner–Boore distance  $R_{jb}$  is used in BSSA14 and the other four GMPEs rupture distance is used. I14 is only limited within  $R_{rup} < 150$  km, however, we extend to 300 km in order to compare with others GMPEs. Comparisons of the observed data with GMPEs developed by the NGA-West2, as shown in Fig. 3, indicated that the median PGA values predicted by NGA-West2 are higher than the partial observed data. Figure 3 presents a comparison between the observed PSAs and the GMPEs developed by NGA-West2. For PSAs at  $T = 0.2$  s, most of the observed values are consistent with the predicted values except the BSSA14, while many of the observed values are beyond one standard deviation away from the predicted values by BSSA14, implying that the BSSA14 results in underpredictions. A majority of the observed PSAs at  $T = 0.5$  and  $1.0$  s are lower than the median values predicted by NGA-West2.

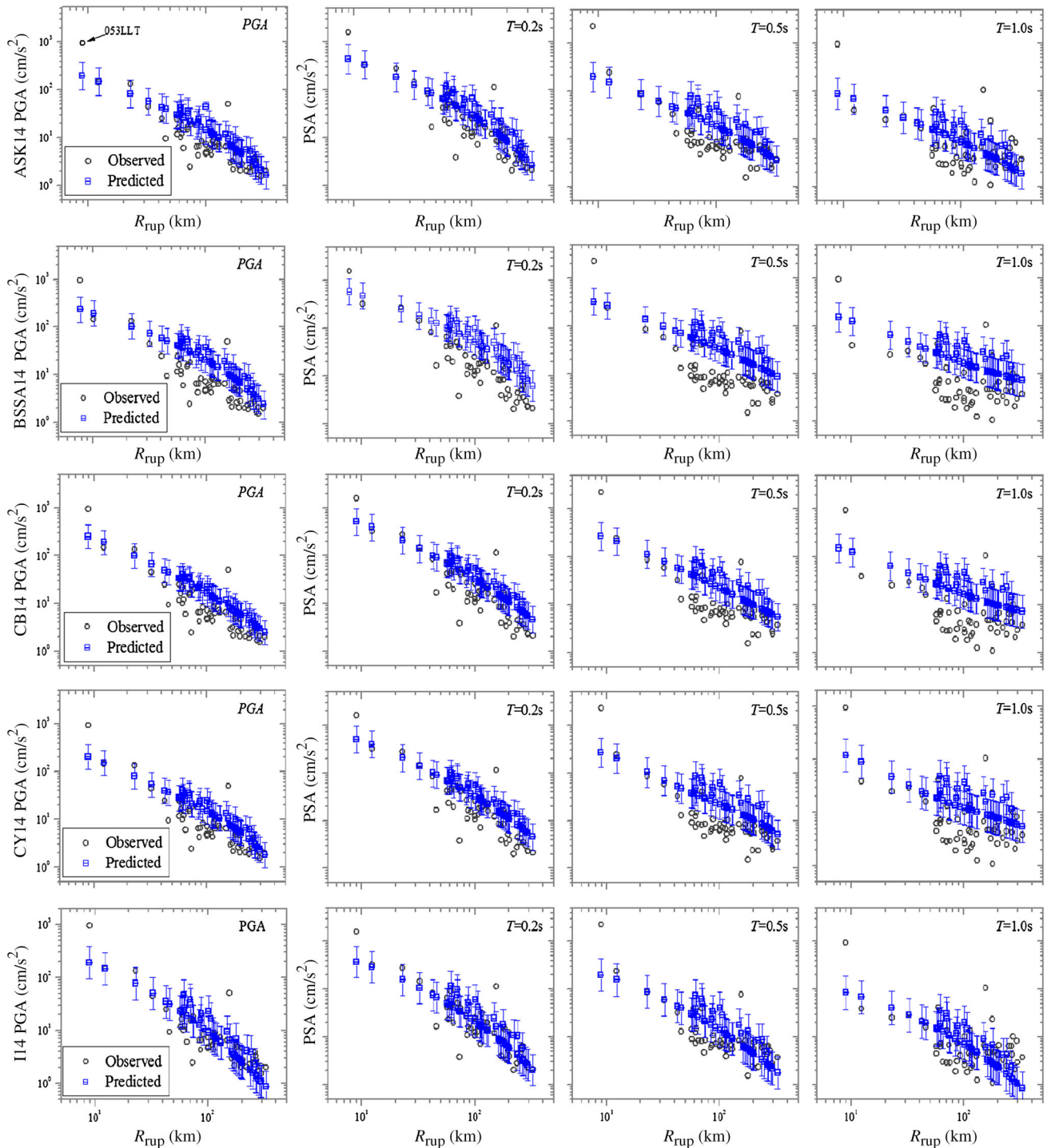


**Fig. 3** Comparison between the observed and predicted horizontal PGAs and 5 % damped pseudo-spectral accelerations at periods  $T = 0.2$ ,  $0.5$ , and  $1.0$  s. The predicted values were calculated using the five NGA-West2 models. *Error bar* denotes the one standard deviation range

#### 4 Comparison of seismic intensity and spectral intensity

Figure 4 shows the isoseismal officially released by China Earthquake Administration (CEA) and seven near-field

strong motion stations in the area of intensity above VI. The maximum intensity is IX, covering the Ludian County and the long axis of isoseismal has northwest–southeast orientation. Table 1 shows the Housner intensity  $I_H$  calculated for the seven stations as shown in Fig. 4, which is

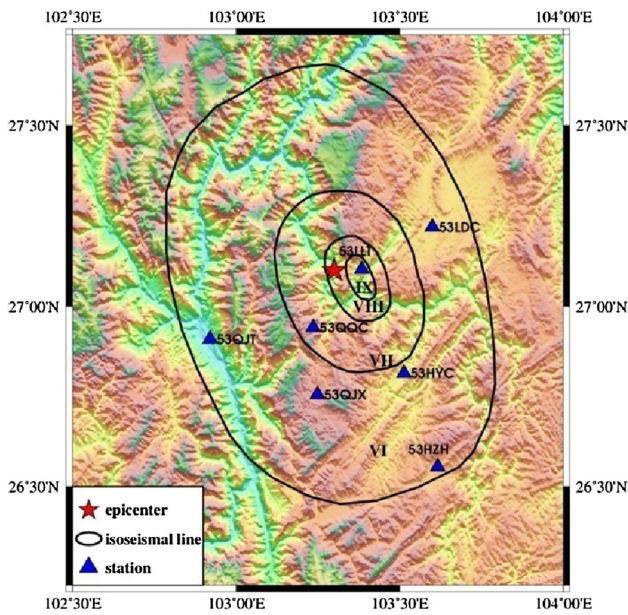


**Fig. 4** The isoseismal released by CEA and seven near-field strong motion stations triggered in the Ludian earthquake. 053LLT station is located within the area of seismic intensity IX

the integral of the velocity response spectrum with different period ranges, 0.1–2.5 s and 0.2–2.0 s (Housner 1952).

The  $I_H$  was also compared with the seismic intensities given by European Macroseismic Scale (EMS) (Grünthal 1998) and Chinese seismic intensity scale, respectively. EMS intensities were estimated by the empirical relationship with  $I_H$  (0.2–2.0 s) proposed by Masi et al. (2011). As shown in Table 1, the intensity under EMS is almost identical to those under Chinese scale. However, results of some stations show a deviation up to one level, which could be mainly explained by specific criteria between these two scales.

### 5 Implications of damage in Longtoushan Town

We investigated the earthquake damage around the strong motion stations where the seismic intensity is greater than VI. 053LLT station is located at the outskirts of

Longtoushan Town of Ludian county where the elevation is 1,577 m.

As shown in Fig. 5, it was found that the buildings around 053LLT station had suffered more serious damages than other stations. The accelerometer is installed on the hard soil site in a bell-shaped housing. The nearby three-story masonry building is out of function, of with the first floor collapsed thoroughly. As shown in Fig. 6a, the duration of strong shaking is only about 5 s, which is relatively short. A large-amplitude pulse is also observed in the acceleration time histories, which will increase the structure response significantly.

The observed horizontal acceleration response spectrum is compared with the design spectrum by the “Code for seismic design of building (GB 50011-2010)” in Fig. 6b. Even though the design spectrum is considered in the case of rare earthquake, the observed spectra are significantly larger than the design spectrum when the period is smaller than 1.5 s ranging the nature period range of common civil buildings in China, which could explain buildings in Longtoushan Town the severe damage.

Masonry is the main structure type for residential housing in the affected area. Figure 7 shows the ruined buildings on both sides of the main road, only about 200 m away from 053LLT station, across the Longtoushan Town. Most of those buildings were vulnerable to ground motions because they did not have seismic designs. In addition, the poor quality of mortar and workmanship also led to the serious damage. Some modern RC buildings were also investigated and we found that they were undamaged or sustained with only slight non-structural damage, which could be seen still standing among the building debris in Fig. 7. This demonstrates the quality and the resistance of construction of these buildings was better than that observed in the masonry residential buildings.

The strong ground shaking also caused the geological disasters, as shown in Figs. 8 and 9. This region is surrounded by mountainous topography with steep slopes. There are some evidences of ongoing pre-earthquake slope instability, but small landslides interpreted to have been caused by the earthquake and appeared to block the road. Tension cracks and lateral spreads adjacent to the river

**Table 1** Seismic intensity under EMS, Chinese scale, and Housner intensity

Seismic scale	053HYC	053HZH	051LDC	053QJT	053QJX	053QJC	053LLT
Chinese seismic intensity	VI	VI	VI	VI	VI	VII	IX
EMS intensity	VI	VI	V	V	VI	VII	X
Natural logarithm of $I_H$ (0.2–2.0 s)	−1.6	−1.6	−2.3	−2.7	−2.0	−1.5	0.9
Natural logarithm of $I_H$ (0.1–2.5 s)	−1.4	−1.5	−2.0	−2.2	−1.8	−1.3	1.1

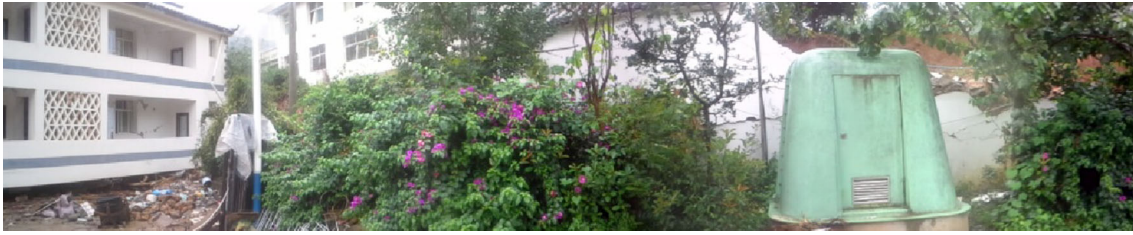


**Fig. 5** The panorama of the 053LLT station. The accelerometer was installed in the *green-color* housing and the three-story masonry building on the left was damaged

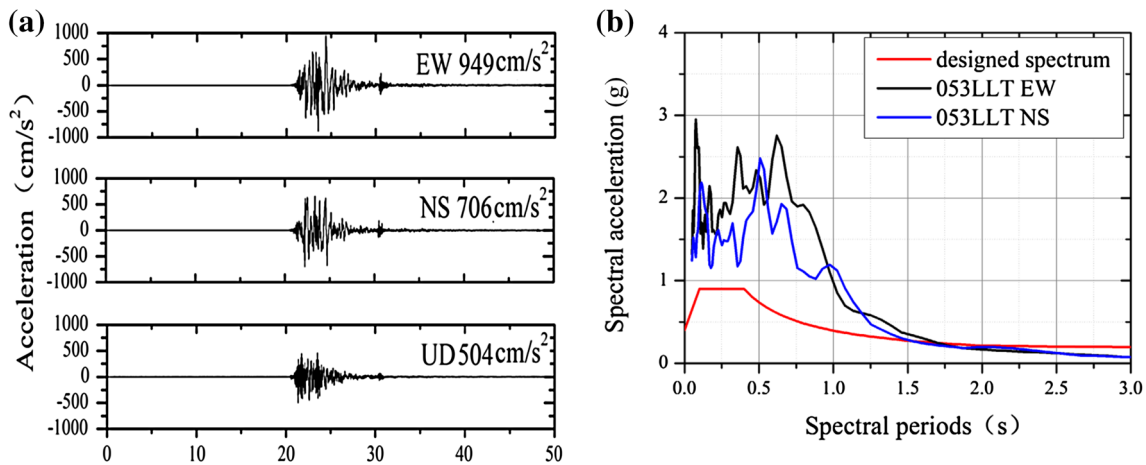


**Fig. 6** **a** Acceleration time histories in the 053LLT station. **b** Comparison of horizontal 5 % damped pseudo-spectral acceleration with Chinese design spectrum



**Fig. 7** Ruined buildings on both sides of the main road across the Longtoushan Town

were also observed. No direct evidence of liquefaction was observed.

## 6 Discussion

Comparisons of the PSAs indicate that the modified NGA models seem favorable to the observed data at short period  $T = 0.2$  s, for the medium and longer periods of 0.5 and 1.0 s, the GMPEs overpredict data. The earthquake damage surrounding the surveyed 053LLT stations is consistent with the issued seismic intensity, though their recorded PGAs are unexpectedly large. However, the recorded ground-motion

hazard levels were considerably higher at 053LLT station and it is most likely that a combination of geological and strong motion effects causing unexpected damage. Although the NGA-West1 has considered the strong motion recordings in the Wenchuan earthquake, there is still not a great improvement of the performance of the NGA-West2 in this test case.

As shown in Figs. 5, 6, 7, 8, and 9, it appears that the extent of damage can be attributed to the existence of a large inventory of structures with deficient capacity and ductility and significant, short-duration velocity pulses with dominant frequencies similar to the fundamental frequencies of typical buildings in the region which have a strong correlation with the seismic intensity.



**Fig. 8** A small landslides blocked the bridge on the road to the Longtoushan Town



**Fig. 9** Collapse of the river bank in Longtoushan Town

## 7 Conclusions

Following a brief review of strong motions and field survey, some conclusions could be drawn for Ludian earthquake:

- (1) The total of 68 groups of strong motion recordings obtained in Ludian earthquake were selected for GMPEs comparison in this paper. For Chinese Huo89, it shown the observed PGAs and PSAs at  $T = 0.2, 0.5,$  and  $1.0$  s are lower than the predicted values in terms of the soil site. For NGA-West2, these recordings contributed to make a comparison of the NGA-West2 as the first case in China. This comparison is useful for understanding the general characteristic of the Ludian earthquake ground motion and for validating predictive models exploiting data sets in China and worldwide. It implies that the observed data are lower than the predicted values by NGA-West2 GMPEs.
- (2) Housner intensity  $I_H$  is calculated for seven near-field strong motion stations. The empirical distribution of

spectral intensity with respect to the seismic intensity under the Chinese scale is almost identical to that under the European scale. The post-earthquake field survey also supported this result.

- (3) The comparison of the observed response spectra and the designed spectrum shows that the observed values are considerably greater than the designed values. The higher than expected strong motion levels caused the serious damage. Poor qualities and lack of maintenance in the buildings could be the reason of great casualty and economic loss.

**Acknowledgments** This work was supported by the Science Foundation of Institute of Engineering Mechanics, China Earthquake Administration (CEA) under Grant No. 2014B06 and the National Natural Science Foundation of China Nos. 51308515 and 51278473. The authors appreciate Prof. Jianwen Cui and his colleagues from Earthquake Administration of Yunnan Province, China for their help in the work of field survey.

**Open Access** This article is distributed under the terms of the Creative Commons Attribution License which permits any use, distribution, and reproduction in any medium, provided the original author(s) and the source are credited.

## References

- Abrahamson NA, Silva WJ, Kamai R (2014) Summary of the ASK14 ground-motion relation for active crustal regions. *Earthq Spectra* 30(3):1024–1056. doi:[10.13/070913EQS8M](https://doi.org/10.13/070913EQS8M)
- Boore DM (2001) Effect of baseline corrections on displacements and response spectra for several recordings of the 99 Chi-Chi, Taiwan, earthquake. *Bull Seismol Soc Am* 91(5):19–1211
- Boore DM, Stewart JP, Seyhan E, Atkinson GM (2014) NGA-West2 equations for predicting PGA, PGV, and 5%-damped PSA for shallow crustal earthquakes. *Earthq Spectra* 30(3):1057–1086. doi:[10.13/070913EQS184M](https://doi.org/10.13/070913EQS184M)
- Campbell KW, Bozorgnia Y (2014) NGA-West2 ground motion model for the average horizontal components of PGA, PGV, and 5%-damped linear acceleration response spectra. *Earthq Spectra* 30(3):1087–1116. doi:[10.13/070913EQS175M](https://doi.org/10.13/070913EQS175M)
- Chiou BSJ, Youngs RR (2014) Update of the Chiou and Youngs NGA model for the average horizontal component of peak ground motion and response spectra. *Earthq Spectra* 30(3):1117–1154. doi:[10.13/070913EQS2M](https://doi.org/10.13/070913EQS2M)
- Gregor N, Abrahamson NA, Atkinson GM, Boore DM, Bozorgnia Y, Campbell KW, Chiou BS-J, Idriss IM, Kamai Ronnie, Seyhan Emel, Silva Walter, Stewart JonathanP, Youngs Robert (2014) Comparison of NGA-West2 GMPEs. *Earthq Spectra* 30(3):1179–18. doi:[10.13/070113EQS186M](https://doi.org/10.13/070113EQS186M)
- Grünthal G (ed) (1998) European Macroseismic Scale 1998 (EMS-98). European Seismological Commission, subcommission on Engineering Seismology, working Group Macroseismic Scales, vol 15. Conseil de l'Europe, Cahiers du Centre Européen de Géodynamique et de Séismologie, Luxembourg
- Hao JL, Wang WM, Yao ZX (2014) [http://www.gg.cas.cn/xwzx/kyjz/201408/r20140808\\_4172104.html](http://www.gg.cas.cn/xwzx/kyjz/201408/r20140808_4172104.html). Accessed 20 Aug 2014
- Housner G (1952) Intensity of ground motion during strong earthquakes. Second technical report. California Institute of Technology, Pasadena

- Hu YX, Zhang MZ (1983) Study on the attenuation law of strong earthquake ground motion near the source. Ph.D Dissertation, Institute of Engineering Mechanism, China Earthquake Administration, Harbin, China (in Chinese with English abstract)
- Huo JR (1989) Study on the attenuation laws of strong earthquake ground motion near the source. Ph.D Dissertation, Institute of Engineering Mechanics, China Earthquake Administration, Harbin (in Chinese with English abstract)
- Idriss IM (2014) An NGA-West2 empirical model for estimating the horizontal spectral values generated by shallow crustal earthquakes. *Earthq Spectra* 30(3):1155–1178. doi:[10.13/070613EQS5M](https://doi.org/10.13/070613EQS5M)
- Masi A, Chiauzzi L, Braga F, Mucciarelli M, Vona M, Ditommaso R (2011) Peak and integral seismic parameters of L'Aquila 2009 ground motions: observed versus code provision values. *Bull Earthq Eng* 9(1):139–156
- Ren YF, Wen RZ, Zhou BF (2011) Cataloging strong-motion recordings—an example of Wenchuan mobile strong-motion observation. *Technol Earthq Disaster Prev* 6(4):406–415 (in Chinese with English abstract)
- Wen RZ, Ren YF, Huang XT, Lu T, Qi WH (2013) Strong motion records and their engineering damage implications for Lushan Earthquake on April 20. *J Earthq Eng Eng Vib* 33(4):1–14 (in Chinese with English abstract)
- Zhang GW, Lei JS, Liang SS, Sun CQ (2014) Relocations and focal mechanisms solutions of the 3 August 2014 Ludian, Yunnan  $M_s$ 6.5 earthquake sequence. *Chin J Geophys* 9(57):3018–3027